

See discussions, stats, and author profiles for this publication at: <https://www.researchgate.net/publication/7169028>

# Bridging the Gap between the Topological and Orbital Description of Hydrogen Bonding: The Case of the Formic Acid Dimer and Its Sulfur Derivatives

ARTICLE in THE JOURNAL OF PHYSICAL CHEMISTRY A · MAY 2006

Impact Factor: 2.69 · DOI: 10.1021/jp057139m · Source: PubMed

CITATIONS

4

READS

22

6 AUTHORS, INCLUDING:



**Soledad Gutiérrez-Oliva**

Pontifical Catholic University of Chile

47 PUBLICATIONS 745 CITATIONS

SEE PROFILE



**Felipe A Bulat**

Pontifical Catholic University of Chile

30 PUBLICATIONS 1,163 CITATIONS

SEE PROFILE



**José H Zagal**

University of Santiago, Chile

197 PUBLICATIONS 3,976 CITATIONS

SEE PROFILE



**Alejandro Toro-Labbé**

Pontifical Catholic University of Chile

223 PUBLICATIONS 4,325 CITATIONS

SEE PROFILE

# Bridging the Gap between the Topological and Orbital Description of Hydrogen Bonding: The Case of the Formic Acid Dimer and Its Sulfur Derivatives

Soledad Gutiérrez-Oliva,<sup>†</sup> Laurent Joubert,<sup>‡</sup> Carlo Adamo,<sup>‡</sup> Felipe A. Bulat,<sup>†</sup> José H. Zagal,<sup>§</sup> and Alejandro Toro-Labbé<sup>\*,†</sup>

Laboratorio de Química Teórica Computacional (QTC), Facultad de Química, Pontificia Universidad Católica de Chile, Casilla 306, Correo 22, Santiago, Chile, Laboratoire d'Electrochimie et Chimie Analytique, UMR CNRS 7575, École Nationale Supérieure de Chimie de Paris, 11 rue P. et M. Curie, F-75231 Paris Cedex 05, France, and Facultad de Química y Biología, Universidad de Santiago de Chile, Casilla 40, Correo 33, Santiago, Chile

Received: December 7, 2005; In Final Form: February 20, 2006

Several molecular descriptors, based on topological approaches as well as on a more traditional orbital-based decomposition, have been used to assess relations with hydrogen bond strengths in a series of formic acid dimers and its sulfur derivatives. Particular attention has been devoted to the analysis of the core-valence bifurcation topological index and to the bond order index. Their values are seen to be linearly related to bond energies estimated through a bond-energy–bond-order relationship; also, the mean value of the topological index appears to be related to the complexation energy computed by methods based on density functional theory. The dependence of the index upon the donor–acceptor couple in relation to its applicability is discussed.

## 1. Introduction

Hydrogen bonds (HB) play a very important role in the study of chemical and biochemical species. Indeed, both structure and reactivity of hydrogen bonded complexes has been an active research field for several decades, in many cases prototype systems have been used, as their study aids in the qualitative and quantitative understanding of more complex systems.<sup>1,2</sup> Nevertheless, as often is the case in chemistry, a commonly used chemical concept—here H-bonding—is based on a qualitative definition; it is therefore not surprising the large amount of literature devoted to more rigorous definitions, both in chemical and in mathematical terms (see, for instance, refs 3–6).

The electron localization function (ELF),<sup>7–9</sup> in particular, has been used as a probe to define the strength of the hydrogen bonds. Denoted hereafter  $\eta(\mathbf{r})$ , this bounded function allows us to separate regions of the real space where electrons are strongly localized (upper limit = 1) from those where the electrons are delocalized (lower limit = 0). A topological partition of the ELF gradient vector field ( $\nabla\eta(\mathbf{r})$ ) provides clear divisions of the molecular space into chemically meaningful regions called topological basins.<sup>8,9</sup> We find two main types of basins: the core and valence basins. Valence basins are characterized by their synaptic order, which specifies the number of core basins with which they share a common boundary. Accordingly, a valence basin can be monosynaptic (lone pairs), disynaptic (two-center bond) or polysynaptic (multicenter bond). A proton is a particular case, counting as a formal core. If this proton is located in a valence basin of another atom, the synaptic order of this basin is therefore increased by one. To quantify the strength of the HBs, Silvi and co-workers introduced a few years ago<sup>5,6</sup> the so-called core-valence bifurcation (CVB) index for the D–H···A hydrogen bond, where D and A correspond to

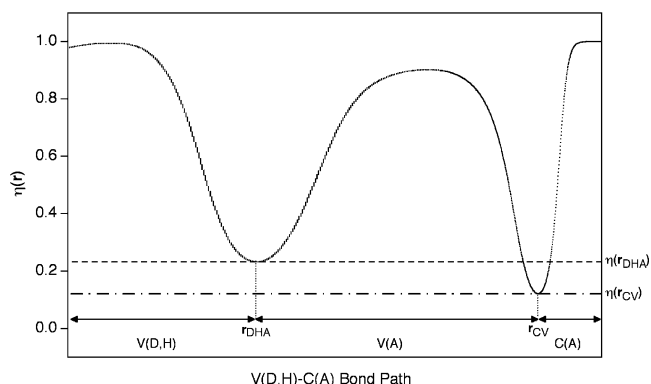


**Figure 1.**  $\eta(\mathbf{r})$  value along the bond path for a prototype D–H···A bond. The CVB (see eq 1 and the text above for details) corresponds to the difference between  $\eta(\mathbf{r}_{\text{DHA}})$  and  $\eta(\mathbf{r}_{\text{CV}})$ .

the donor and acceptor atoms, respectively. Figure 1 shows the  $\eta(\mathbf{r})$  value along a typical D–H···A bond path, the CVB corresponds to the difference between  $\eta(\mathbf{r}_{\text{DHA}})$ , the value of the saddle connection of the  $V(\text{D,H})$  and  $V(\text{A})$  basins, and  $\eta(\mathbf{r}_{\text{CV}})$ , the lowest value of the ELF for which all the core basins of the complex are separated from the valence:

$$\text{CVB}_{(\text{DHA})} = \eta(\mathbf{r}_{\text{DHA}}) - \eta(\mathbf{r}_{\text{CV}}) \quad (1)$$

Negative values of CVB indicates a weak interaction between the two moieties D–H and A, this interaction is physically interpreted as being mostly of electrostatic nature. On the other hand, a positive CVB indicates a moderate interaction where the main electrostatic nature of the HB is preserved but an additional covalent interaction, due to the electronic delocalization between the  $V(\text{D,H})$  and  $V(\text{A})$  basins, emerges. Silvi and co-workers<sup>5,6</sup> found a linear relationship between the CVB index and the complexation energy for a series of HBs of different strength, where in all cases fluorine was the donor atom. Indeed, both the complexation energies and the stretching harmonic

\* To whom correspondence should be addressed. E-mail: atola@puc.cl.

<sup>†</sup> Pontificia Universidad Católica de Chile.

<sup>‡</sup> École Nationale Supérieure de Chimie de Paris.

<sup>§</sup> Universidad de Santiago de Chile.

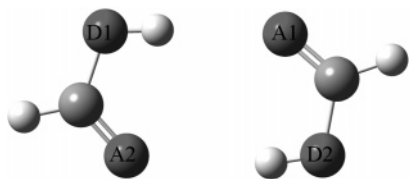


**Figure 2.** Sketch of the prototype doubly hydrogen bonded complexes. The donor–acceptor couples (DA) are shown in Table 1, where it is seen that for the present study D and A are either sulfur or oxygen.

frequency shifts, used as an experimental criteria for the HB strength, display linear relationships with respect to the CVB index, indicating that “the topological and the experimentalist’s criteria form consistent and complementary tools for the characterization of the hydrogen-bond strength”.<sup>5,6</sup>

In the present study, we further analyze the application of the CVB topological index in HBs, by considering a series of doubly hydrogen bonded complexes. Formic acid dimers and its sulfur derivatives were chosen as prototype systems (Figure 2).<sup>14</sup> Formic acid dimers, which exist in formic acid vapors even at room temperature, and some of their derivatives, are among the most studied prototype complexes.<sup>10</sup> Several experimental<sup>11–13</sup> as well as theoretical studies<sup>2,14–18</sup> address energetic and structural features of hydrogen bonded complexes as well as the proton-transfer reactions they undergo, shedding much light on their intrinsic properties and mechanisms.

Because each HB is characterized through its donor–acceptor couple (oxygen and sulfur), the model systems chosen in this work give the possibility of studying four types of HBs under different environments. The four types of HBs we are dealing with in this paper are O–H···O, O–H···S, S–H···O, and S–H···S. The complexation energies, directly obtained by density functional theory (DFT) calculations, are compared with the (CVB) index which is the average of the individual CVBs associated to each HBs on the complex. Then, to have a more complete picture of the H-bond interaction and to bridge the gap between topological and orbital indexes, bond energies estimated using an orbital approach, such as the bond-energy–bond-order (BEBO) model,<sup>19</sup> are compared with the CVB values for each bond. Because the donor and acceptor atoms involved on each HB are allowed to change, a complete analysis on the effect of the donor–acceptor couple on the CVB index is obtained, thus giving more insight on the usage and interpretation of the CVB index and its direct relationship with the BEBO model.

## 2. Computational Methods

Figure 2 sketches the prototype systems studied, spanning all possible dimers formed out of the HCXXH, X = O, S monomers. The donor–acceptor couples for the HBs for each complex along their numbering are shown in Table 1.

All calculations were performed using the Gaussian 98<sup>20</sup> and Gaussian 03<sup>21</sup> programs. All the structures of the four monomers (HCXXH, X = O, S) and the 10 dimers were optimized using the PBE0 hybrid exchange–correlation functional,<sup>22,23</sup> with a split valence double- $\zeta$  basis (6-31G(d,p)) augmented with polarization functions on both heavy and hydrogen atoms. Frequency calculations were performed to check that all the geometries correspond to energy minima. Wave functions were then obtained at the same level so as to perform the ELF topological analysis using a local code, derived from the TopMod suite of programs,<sup>24</sup> to obtain the CVB index.<sup>5,6</sup> A modified version of Gaussian 98’s Link 601, developed by one of the authors,<sup>25</sup> was used to obtain the bond orders (BOs), as defined in refs 26 and

**TABLE 1: Core-Valence Bifurcation Index, Donor–Hydrogen (D–H), Hydrogen–Acceptor (H···A), and Donor–Acceptor (D–H···A) Distances and Bond Order for Each Hydrogen Bond on Each Dimer<sup>a</sup>**

	bond type	CVB	$r(\text{D–H})$	$r(\text{H···A})$	$r(\text{D–H···A})$	BO
C1	O–H···O (1,1)	−0.111	1.0082	1.6051	2.6133	0.1645
	O–H···O (2,1)	−0.111	1.0082	1.6051	2.6133	0.1645
C2	O–H···O (3,1)	−0.054	0.9934	1.6984	2.6918	0.1340
	S–H···O (4,3)	−0.054	1.3730	1.8237	3.1967	0.0983
C3	O–H···S (5,2)	−0.174	1.0009	2.1481	3.1490	0.2145
	O–H···O (6,1)	−0.110	1.0082	1.5929	2.6011	0.1641
C4	O–H···S (7,2)	−0.118	0.9917	2.2373	3.2290	0.1663
	S–H···O (8,3)	−0.045	1.3711	1.8400	3.2111	0.0949
C5	S–H···O (9,3)	−0.005	1.3614	1.9441	3.3055	0.0730
	S–H···O (10,3)	−0.005	1.3614	1.9441	3.3055	0.0730
C6	O–H···S (11,2)	−0.168	1.0005	2.1519	3.1524	0.2124
	O–H···S (12,2)	−0.168	1.0005	2.1519	3.1524	0.2124
C7	S–H···S (13,4)	−0.153	1.3788	2.3003	3.6791	0.1291
	O–H···O (14,1)	−0.061	0.9960	1.6738	2.6698	0.1381
C8	S–H···O (15,3)	−0.004	1.3616	1.9418	3.3034	0.0719
	S–H···S (16,4)	−0.076	1.3672	2.4313	3.7985	0.0907
C9	O–H···S (17,2)	−0.121	0.9936	2.2231	3.2167	0.1716
	S–H···O (18,4)	−0.126	1.3758	2.3386	3.7144	0.1181
C10	S–H···S (19,4)	−0.067	1.3675	2.4442	3.8117	0.0883
	S–H···S (20,4)	−0.067	1.3675	2.4442	3.8117	0.0883

<sup>a</sup> The numbers in parenthesis next to the donor–acceptor couple represent the individual HB numbering and its type. All distances are in angstroms.

27 for an arbitrary X–Y bond out of a closed shell wave function:

$$\text{BO}_{\text{X–Y}} = \sum_{\mu \in \text{X}} \sum_{\nu \in \text{Y}} \left\{ \left\{ \sum_k P_{\mu,k} S_{k,\nu} \right\} \left\{ \sum_k P_{\nu,k} S_{k,\mu} \right\} \right\} \quad (2)$$

where the symbols  $P$  and  $S$  are the density and overlap matrices; the innermost sum goes through all  $K$  basis functions whereas the outer sums go through all those centered in X or Y, respectively. For the HB cases D–H···A, we estimate  $\text{BO}_{\text{H···A}}$  through eq 2 above, although we will drop the subscript H···A for typographical convenience.

To study the individual HBs’ energies as a function of the CVB topological index, a bond-energy–bond-order (BEBO) resolution of the complexation energy was performed. The model used for the BEBO relation is the following second-order polynomial relationship

$$E_b(i)(\text{BO}_i; D_i, P_i) = D_i \left[ \frac{2\text{BO}_b}{P_i} + \left( \frac{\text{BO}_b}{P_i} \right)^2 \right] = \frac{2D_i}{P_i} \text{BO}_b + \frac{D_i}{P_i^2} (\text{BO}_b)^2 \quad (3)$$

which is similar to that of ref 28; here the parameters  $D_i$  and  $P_i$  do not have any physical meaning, they are just fitting parameters. This equation is indeed that obtained when using the bond order as defined by Pauling<sup>29</sup> in the equation proposed by Johnston and Parr,<sup>19</sup> yielding a BEBO relationship.

In eq 3 above,  $E_b(i)$  is the energy of the  $b$ th HB (of the  $i$ th type),  $D_i$  and  $P_i$  are the fit parameters for the corresponding bond type. As 10 complexes are studied but only four types of HBs are present (yielding a total of eight fit parameters), an overdetermined system of equations has to be solved. Each equation represents the total complexation energy for each complex as the sum of the two HBs’ individual energies. For example, the complex labeled C2 in Table 1 yields a complexation energy  $\Delta E_{\text{C2}} = E_3(1) + E_4(3)$ . The system of 10 equations for  $\Delta E_{\text{C}}$  (one for each complexation energy) is dealt with by

**TABLE 2: Mean CVB, Donor–Hydrogen (D–H), Hydrogen–Acceptor (H···A), and Donor–Acceptor (D–H···A) Mean Distances, Mean BO and Complexation Energy for Each Dimer<sup>a</sup>**

	CVB	$\bar{r}(\text{D–H})$	$\bar{r}(\text{H}\cdots\text{A})$	$\bar{r}(\text{D–H}\cdots\text{A})$	BO	$\Delta E_c$
C1	−0.111	1.0082	1.6051	2.6133	0.1645	−17.0683
C2	−0.054	1.1832	1.7611	2.9443	0.1161	−10.9814
C3	−0.142	1.0046	1.8705	2.8751	0.1893	−14.9975
C4	−0.081	1.1814	2.0387	3.2201	0.1306	−9.6637
C5	−0.005	1.3614	1.9441	3.3055	0.0730	−6.5261
C6	−0.168	1.0005	2.1519	3.1524	0.2124	−12.4247
C7	−0.107	1.1874	1.9871	3.1745	0.1336	−10.5422
C8	−0.040	1.3644	2.1866	3.5510	0.0813	−6.3379
C9	−0.124	1.1847	2.2809	3.4656	0.1449	−8.8479
C10	−0.067	1.3675	2.4442	3.8117	0.0883	−5.7731

<sup>a</sup> All distances are in angstroms, energies in kcal/mol.

solving all possible combinations of eight equations with eight unknowns by systematically discarding two equations. For each time the system of eight equations is solved, the error in the estimation of the complexation energy for the eight considered complexes will be zero, but there will be a nonzero error in the estimation of the complexation energies of the remaining two complexes. The root-mean-squared deviation in the estimation of the 10 complexation energies for each time the  $8 \times 8$  systems is solved, is calculated and a weight  $\omega_i$  is assigned using a Gaussian distribution with a given variance  $\sigma$  (and zero mean). The solution sets  $\{D, P\}_i$  are used to obtain a weighted set of parameters that yields a given error as a function of  $\sigma$  ( $\{D(\sigma), P(\sigma)\} = \sum \omega_i(\sigma) \{D, P\}_i / \sum \omega_i(\sigma)$ ). Finally,  $\sigma$  is chosen to produce the set of fit parameters that yield the minimal statistical error.

### 3. Results and Discussion

In Table 1 we collect, along with the numbering and bond types for each complex, the CVB indexes, donor–hydrogen ( $\bar{r}(\text{D–H})$ ), hydrogen–acceptor ( $\bar{r}(\text{H}\cdots\text{A})$ ) and donor–acceptor ( $\bar{r}(\text{D–H}\cdots\text{A})$ ) distances as well as the bond order for the HBs in each complex. In Table 2 these data are summarized taking their mean value and complemented with the DFT complexation energy ( $\Delta E_c$ ) for each system, calculated as the difference between the complex energy and that of the free monomers. These last values are corrected for the basis set superposition error (BSSE) through the counterpoise method.<sup>30</sup>

Figure 3 shows the complexation energies against the mean interatomic distances of the atoms involved in the HBs, this is the donor–hydrogen ( $\bar{r}(\text{D–H})$ , upper panel), hydrogen–acceptor ( $\bar{r}(\text{H}\cdots\text{A})$ , middle panel) and donor–acceptor ( $\bar{r}(\text{D–H}\cdots\text{A})$ , lower panel) distances. It is evident from these plots that three different groups can be identified. Indeed, the complexes C1, C3 and C6 form group **A**, complexes C2, C4, C7 and C9 form group **B**, whereas complexes C5, C8 and C10 form group **C**. This behavior can be easily rationalized in terms of the donor atom: in group **A** the donor on both HBs is oxygen; in group **C** the donor is sulfur and in group **B**, the donor is oxygen for one bond and sulfur for the other.

This grouping well highlights the importance of the donor atom in ruling the properties of the HBs, it must be noted that the donor–hydrogen distance remains quite constant within each group (see Figure 3a). On the other hand, a linear relationship between the average hydrogen–acceptor distances and the complexation energy is found (Figure 3b) for each group of complexes. This relation is particularly interesting because the bond orders (through Pauling's formula<sup>29</sup>), and hence the bond energies, are directly related to this distance. Finally, the same grouping can be found when the DFT complexation energies

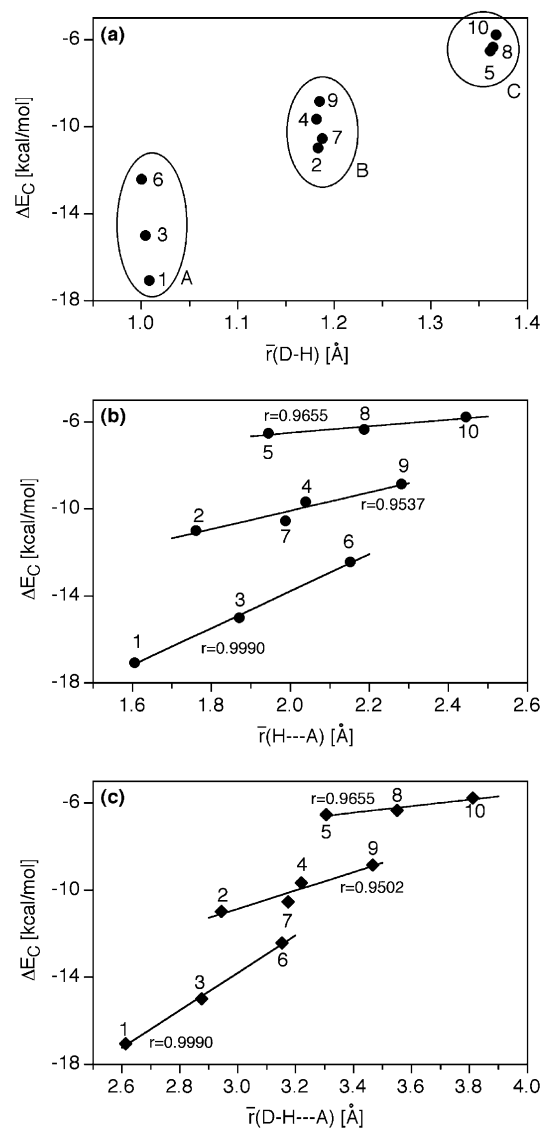


**Figure 3.** Complexation energy against (a) mean donor–hydrogen distance, (b) mean acceptor–hydrogen distance and (c) mean donor–acceptor distance. For each straight line shown the correlation coefficient is displayed. Next to each point the numbering of the complex as in Table 1 is shown.

are plotted against the overall donor–hydrogen–acceptor distance (see Figure 3c). In all cases correlation coefficients ( $r$ ) close to 1 are obtained.

Although these relationships for the mean distances out of Figure 3 are not completely unexpected, but quite natural actually, it is interesting to note that such grouping is also recovered when different HB descriptors are considered. Figure 4 shows the relationship between the CVB index and the mean hydrogen–acceptor distance (Figure 4a), the total complexation energy (Figure 4b) and the mean bond-order (Figure 4c). The same grouping ( $\{C1, C3, C6\}; \{C2, C4, C7, C9\}; \{C5, C8, C10\}$ ) can be easily identified in each plot. Again, for the CVB against  $\bar{r}(\text{H}\cdots\text{A})$  plot, this grouping is quite natural, but the linear relationships shown for the energy and mean BO against CVB for each group of complexes are quite remarkable. It can also be observed that the mean BO and energy against CVB plots for group **B**, having one O–H···X and one S–H···X bonds, are approximately the mean of those for groups **A** and **C** that present only O–H···X and S–H···X bonds, respectively. Particularly noteworthy is the comparison of the energy and

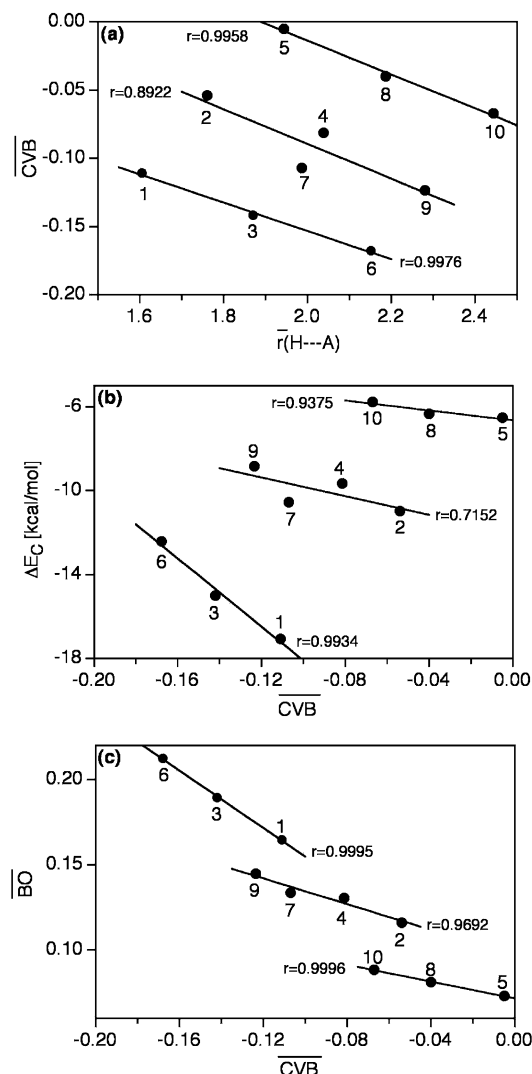


**Figure 4.** Relationships between the mean CVB index against (a) mean hydrogen–acceptor distance, (b) complexation energy and (c) mean bond order. For each straight line shown the correlation coefficient is displayed. Next to each point the numbering of the complex as in Table 1 is shown.

mean BO relations with the CVB index. As both present a linear behavior for each group, it can be inferred that there will be an approximate linear relationship between the energy and the mean BOs and hence also between the individual bond energies and BOs.

Figure 5 shows relations between the CVB, bond order and hydrogen–acceptor distance for each HB. We note from Figure 5a that there is a linear relationship between the bond order and the CVB index when keeping the donor atom fixed. In Figure 5b, linear relationships are obtained for the CVB against the hydrogen–acceptor distance when keeping the acceptor atom fixed. Therefore, these data show an unexpected linear relation between the CVB index with both the BO descriptor and the structural property  $r(\text{H}\cdots\text{A})$ . It must also be pointed out that the previous grouping is no longer reproduced in these plots. Instead, the data can be divided in two main groups, depending on the acceptor atom involved in the HBs (oxygen or sulfur). Finally, Figure 5c indicates that within the relatively narrow bond-order range spanned by the studied bonds, the relationship between BO and  $r(\text{H}\cdots\text{A})$  is, as expected from eq 2, approximately linear.

Most of the previous analysis could be complemented by the plots of the individual HB energies against the CVB index. This

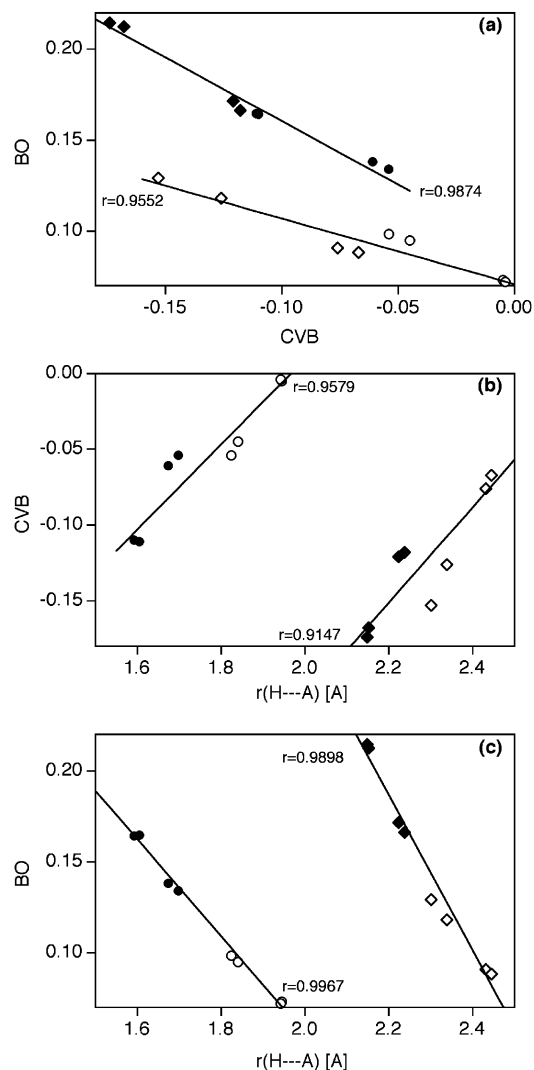


**Figure 5.** Plots for (a) bond order against the CVB index, (b) hydrogen–acceptor distance against CVB index and (c) hydrogen–acceptor distance against bond order. The filled symbols are for the O–donor bonds (O–H $\cdots$ O, ●; O–H $\cdots$ S, ◆), and the hollow ones are for the S–donor bonds (S–H $\cdots$ O, ○; and S–H $\cdots$ S, ◇). Note also the O–acceptor cases are represented by circles (● and ○), whereas the S–acceptor cases are represented by diamonds (◆ and ◇).

last comparison will allow us not only to have a direct comparison with the observations of Silvi and co-workers<sup>5,6</sup> but also to extend them. In particular, it will be interesting to evidence a linear relationship for the bond energy as a function of the CVB index, thus complementing the experimental criteria for the HB strength.

As already mentioned, a BEBO resolution of the complexation energies was made, considering two HB energies for each complex. Table 3 summarizes these results, collecting the estimated bond energy from the BEBO analysis along with the CVB index. The absolute error made in estimating the DFT complexation energy  $\Delta E_c$  as the sum of the individual bond energies  $E^b$  is shown in the rightmost column. Note that because of the overdetermined nature of the equation system, the sum of the two bond energies  $E^b$  is only approximately the DFT complexation energy  $\Delta E_c$ . The root-mean-squared sum of the absolute errors yields the minimal statistical error described previously.

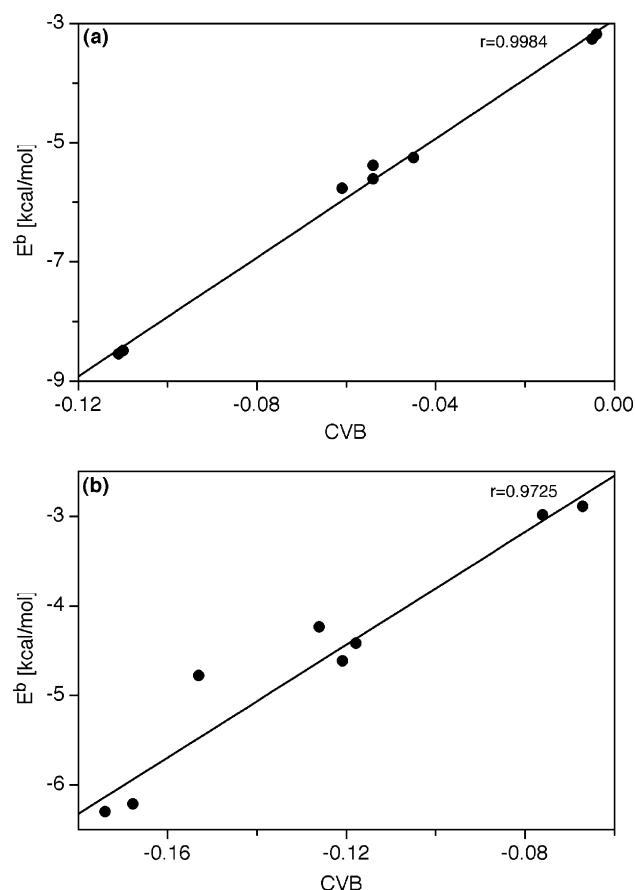
Figure 6 shows the BEBO-resolved HB energies as a function of the CVB index, for both the X–H $\cdots$ O (oxygen as acceptor, upper panel) and X–H $\cdots$ S (sulfur as acceptor, lower panel)



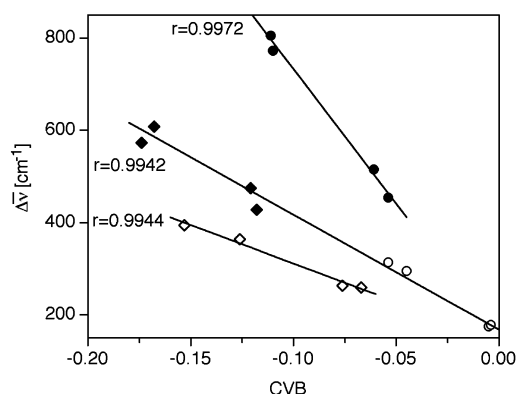
**TABLE 3: CVB Index and Hydrogen Bond Energies for Each Hydrogen Bond<sup>a</sup>**

	bond type	CVB	$E^b$	error
C1	O—H...O	-0.111	-8.5360	0.0037
	O—H...O	-0.111	-8.5360	
C2	O—H...O	-0.054	-5.3832	0.0046
	S—H...O	-0.054	-5.6029	
C3	O—H...S	-0.174	-6.2998	0.2106
	O—H...O	-0.101	-8.4872	
C4	O—H...S	-0.118	-4.4186	0.0034
	S—H...O	-0.045	-5.2485	
C5	S—H...O	-0.005	-3.2651	0.0041
	S—H...O	-0.005	-3.2651	
C6	O—H...S	-0.168	-6.2125	0.0003
	O—H...S	-0.168	-6.2125	
C7	S—H...S	-0.153	-4.7779	0.0013
	O—H...O	-0.061	-5.7655	
C8	S—H...O	-0.004	-3.1804	0.1731
	S—H...S	-0.076	-2.9844	
C9	O—H...S	-0.121	-4.6131	0.0001
	S—H...S	-0.126	-4.2349	
C10	S—H...S	-0.067	-2.8866	0.0000
	S—H...S	-0.067	-2.8866	

<sup>a</sup> Energies were calculated out of the complexation energy for each complex and bond orders in Table 2, resorting to the BEBO resolution using eq 3. The rightmost column shows the error made when estimating the complexation energy as the sum of the bebo energies for each complex.

**Figure 6.** Bond energies out of the BEBO analysis against the CVB index. The upper (lower) panel shows the cases on which oxygen (sulfur) is the acceptor atom.

bonds. In both cases a linear relationship is seen between the bond energy (as a measure of the bond strength) and the CVB index, further supporting the observations of Silvi and co-workers.<sup>5,6</sup> In our case, the linear relationship is seen to hold when keeping the acceptor atom fixed. Indeed, it should not be

**Figure 7.** Difference in the frequency shifts (plotted as wavenumbers) against the CVB index (O—H...O, ●; O—H...S, ◆; S—H...O, ○; S—H...S, ◇; as in Figure 5). Wavenumbers in reciprocal centimeters.

expected that equivalent linear relationships should hold whichever the donor–acceptor couple is. The linear relations underline the connection between topological and orbital-based analysis for such weak interactions. This connection has been recently observed for other weak chemical interactions.<sup>31</sup>

It should be also noted from Figure 6 that the linear regression is much better when oxygen acts as the acceptor than when sulfur does. This phenomena is considered to be a consequence of the higher polarizability of sulfur, which might be much more affected by the environment than oxygen. It is to be stressed that even for sulfur the results are quite encouraging, and CVB does indeed measure the bond strength.

To assess the relationship between the experimental D–H stretching frequency versus the CVB index as bond strength indicators, we have estimated the difference between the stretching frequency of the monomers and that seen for the dimers. As for each D–H type there are two frequencies, one for each monomer that presents the same D–H group, we have taken the mean  $\nu_{\text{DH}}^0$  as a reference value. An analysis of the normal vibration modes has been performed so as to identify the two D–H bond stretching frequency on each dimer  $\nu_{\text{DH}}^i$ ,  $i = 1, 2, \dots, 20$  (here we follow the numbering shown in Table 1 for each of the 20 HBs). The  $\nu_{\text{DH}}^i - \nu_{\text{DH}}^0$  difference has been plotted in Figure 7 against the CVB index. We observe that good correlation between both indexes is obtained only when moieties of similar masses are compared, which distinguishes three cases: O—H...O (upper curve), S—H...S (lower curve) and O—H...S and S—H...O (middle curve). This splitting of the relationship into groups hinders the direct applicability of the CVB when correlated to the frequency shifts.

#### 4. Concluding Remarks

A study devoted to the description of hydrogen-bond interactions through the use of few molecular descriptors was performed. Linear correlations depending on the nature of both acceptor and donor atoms were obtained between the CVB index, complexation energies and geometrical parameters. Our results show that the mean CVB index is strongly correlated with the complexation energy computed from DFT calculations. Also the individual HB energies, obtained through the BEBO model, show a good linear relationships with the CVB index when the acceptor atom is kept fixed.

Our work confirms that the CVB index is a valuable tool for the estimation of the HB strength while certain conditions are kept fixed. Further work along these lines should clarify this situation, enabling the usage of the CVB topological criteria in complex systems where BEBO resolutions could be difficult

and/or inaccurate and frequency shifts hard to identify. This is indeed the case as electron density and hence the topological CVB indexes are probably more accurate than any of the other possibilities (BEBO resolution or frequency shifts). Moreover, the use of topological indexes based upon the electronic density to describe weak interactions is quite appealing as densities obtained out of low level theoretical calculations for extended systems tend to be reasonably good. From a more general point of view, our results underline the complementarity of different theoretical analysis tools, based on topology or on more traditional molecular orbital approaches.

**Acknowledgment.** We gratefully acknowledge financial support from FONDECYT through projects No. 1060590 and No. 8010006; Project FONDAP No. 11980002 (CIMAT); Programa Bicentenario en Ciencia y Tecnología (PBCT), Project No. 8 (Inserción Académica); Program ECOS-CONICYT C03E02. S.G.-O. acknowledges financial support from Núcleo Milenio de Mecánica Cuántica Aplicada y Química Computacional, Código P02-004-F. C.A. and L.J. wish to thank Laboratorio de Química Teórica Computacional at PUC (QTC@PUC) for the warm hospitality.

## References and Notes

- (1) Pross, A. *Theoretical and Physical Principles of Organic Reactivity*; John Wiley & Sons: New York, 1995.
- (2) Scheiner, S. In *Hydrogen Bonding: A Theoretical Perspective*; Truhlar, D. G., Ed.; Topics in Physical Chemistry; Oxford University Press: New York, 1997.
- (3) Hobza, P.; Havlas, Z. *Chem. Rev.* **2000**, *100*, 4253.
- (4) Koch, U.; Popelier, P. L. A. *J. Phys. Chem.* **1995**, *99*, 9747.
- (5) Fuster, F.; Silvi, B. *Theor. Chem. Acc.* **2000**, *104*, 13.
- (6) Alhikani, M. E.; Fuster, F.; Silvi, B. *Struct. Chem.* **2005**, *16*, 203.
- (7) Becke, A. D.; Edgecombe, K. E. *J. Chem. Phys.* **1990**, *92*, 5397.
- (8) Silvi, B.; Savin, A. *Nature* **1994**, *371*, 683.
- (9) Savin, A.; Silvi, B.; Colonna, F. *Can. J. Chem.* **1996**, *74*, 1088.
- (10) Buckingham, A. D. *NATO ASI Ser. Ser. C* **2000**, *561*, 1.
- (11) Jeffrey, G. A. In *An Introduction to Hydrogen Bonding*; Truhlar, D. G., Ed.; Topics in Physical Chemistry; Oxford University Press: New York, 1997.
- (12) Stöckli, A.; Meier, B. H.; Kreis, R.; Meyer, R.; Ernst, R. R. *J. Chem. Phys.* **1990**, *93*, 1502.
- (13) Matyilitsky, V. V.; Riehn, C.; Gelin, M. F.; Brutschy, B. *J. Chem. Phys.* **2003**, *119*, 10553.
- (14) Jaque, P.; Toro-Labbé, A. *J. Phys. Chem. A* **2000**, *104*, 995.
- (15) Gutiérrez-Oliva, S.; Jaque, P.; Toro-Labbé, A. *J. Phys. Chem. A* **2000**, *104*, 8955.
- (16) Emmeluth, C.; Suhm, M. A.; Luckhaus, D. *J. Chem. Phys.* **2003**, *118*, 2242.
- (17) Pacios, L. F. *J. Phys. Chem. A* **2004**, *108*, 1177.
- (18) Gutiérrez-Oliva, S.; Herrera, B.; Toro-Labbé, A.; Chermette, H. *J. Phys. Chem. A* **2005**, *109*, 1748.
- (19) Johnston, H. S.; Parr, C. J. *Am. Chem. Soc.* **1960**, *85*, 2544.
- (20) Frisch, M. J.; Trucks, G. W.; Schlegel, H. B.; Scuseria, G. E.; Robb, M. A.; Cheeseman, J. R.; Zakrzewski, V. G.; Montgomery, J. A., Jr.; Stratmann, R. E.; Burant, J. C.; Dapprich, S.; Millam, J. M.; Daniels, A. D.; Kudin, K. N.; Strain, M. C.; Farkas, O.; Tomasi, J.; Barone, V.; Cossi, M.; Cammi, R.; Mennucci, B.; Pomelli, C.; Adamo, C.; Clifford, S.; Ochterski, J.; Petersson, G. A.; Ayala, P. Y.; Cui, Q.; Morokuma, K.; Salvador, P.; Dannenberg, J. J.; Malick, D. K.; Rabuck, A. D.; Raghavachari, K.; Foresman, J. B.; Cioslowski, J.; Ortiz, J. V.; Baboul, A. G.; Stefanov, B. B.; Liu, G.; Liashenko, A.; Piskorz, P.; Komaromi, I.; Gomperts, R.; Martin, R. L.; Fox, D. J.; Keith, T.; Al-Laham, M. A.; Peng, C. Y.; Nanayakkara, A.; Challacombe, M.; Gill, P. M. W.; Johnson, B.; Chen, W.; Wong, M. W.; Andres, J. L.; Gonzalez, C.; Head-Gordon, M.; Replogle, E. S.; Pople, J. A. *Gaussian 98*, revision A.11.1; Gaussian, Inc.: Pittsburgh, PA, 2001.
- (21) Frisch, M. J.; Trucks, G. W.; Schlegel, H. B.; Scuseria, G. E.; Robb, M. A.; Cheeseman, J. R.; Montgomery, J. A., Jr.; Vreven, T.; Kudin, K. N.; Burant, J. C.; Millam, J. M.; Iyengar, S. S.; Tomasi, J.; Barone, V.; Mennucci, B.; Cossi, M.; Scalmani, G.; Rega, N.; Petersson, G. A.; Nakatsuji, H.; Hada, M.; Ehara, M.; Toyota, K.; Fukuda, R.; Hasegawa, J.; Ishida, M.; Nakajima, T.; Honda, Y.; Kitao, O.; Nakai, H.; Klene, M.; Li, X.; Knox, J. E.; Hratchian, H. P.; Cross, J. B.; Bakken, V.; Adamo, C.; Jaramillo, J.; Gomperts, R.; Stratmann, R. E.; Yazyev, O.; Austin, A. J.; Cammi, R.; Pomelli, C.; Ochterski, J. W.; Ayala, P. Y.; Morokuma, K.; Voth, G. A.; Salvador, P.; Dannenberg, J. J.; Zakrzewski, V. G.; Dapprich, S.; Daniels, A. D.; Strain, M. C.; Farkas, O.; Malick, D. K.; Rabuck, A. D.; Raghavachari, K.; Foresman, J. B.; Ortiz, J. V.; Cui, Q.; Baboul, A. G.; Clifford, S.; Cioslowski, J.; Stefanov, B. B.; Liu, G.; Liashenko, A.; Piskorz, P.; Komaromi, I.; Martin, R. L.; Fox, D. J.; Keith, T.; Al-Laham, M. A.; Peng, C. Y.; Nanayakkara, A.; Challacombe, M.; Gill, P. M. W.; Johnson, B.; Chen, W.; Wong, M. W.; Gonzalez, C.; Pople, J. A. *Gaussian 03*, revision B.04; Gaussian, Inc.: Wallingford, CT, 2004.
- (22) Adamo, C.; Barone, V. *J. Chem. Phys.* **1999**, *110*, 6158.
- (23) Ernzerhof, M.; Scuseria, G. E. *J. Chem. Phys.* **1999**, *111*, 911.
- (24) Noury, S.; Krokidis, X.; Fuster, F.; Silvi, B. *Comput. Chem.* **1999**, *23*, 597.
- (25) Bulat, F. A.; Chamorro, E.; Fuentealba, P.; Toro-Labbé, A. *J. Phys. Chem. A* **2004**, *108*, 342.
- (26) Mayer, I. *Chem. Phys. Lett.* **1983**, *97*, 270.
- (27) Jensen, F. *Introduction to Computational Chemistry*; John Wiley & Sons: England, 1999.
- (28) Hu, Y. H.; Ruckenstein, E. *Chem. Phys. Lett.* **2004**, *399*, 503.
- (29) Pauling, L. *J. Am. Chem. Soc.* **1947**, *69*, 542.
- (30) Boys, S. F.; Bernardi, F. *Mol. Phys.* **1970**, *19*, 553.
- (31) Petit, L.; Joubert, L.; Maldivi, P.; Adamo, C. *J. Am. Chem. Soc.*, in press.